AD-A078 917 NAVAL RESEARCH LAB WASHINGTON DC F/G 20/4
GAS CHANNEL FORMATION: DEPENDENCE OF HYDRODYNAMIC PHENOMENA ON --ETC(U)
NOV 79 M LAMPE , S KAINER
UNCLASSIFIED NRL-MR-4129 NL

1 OF 1
AD-
A078917

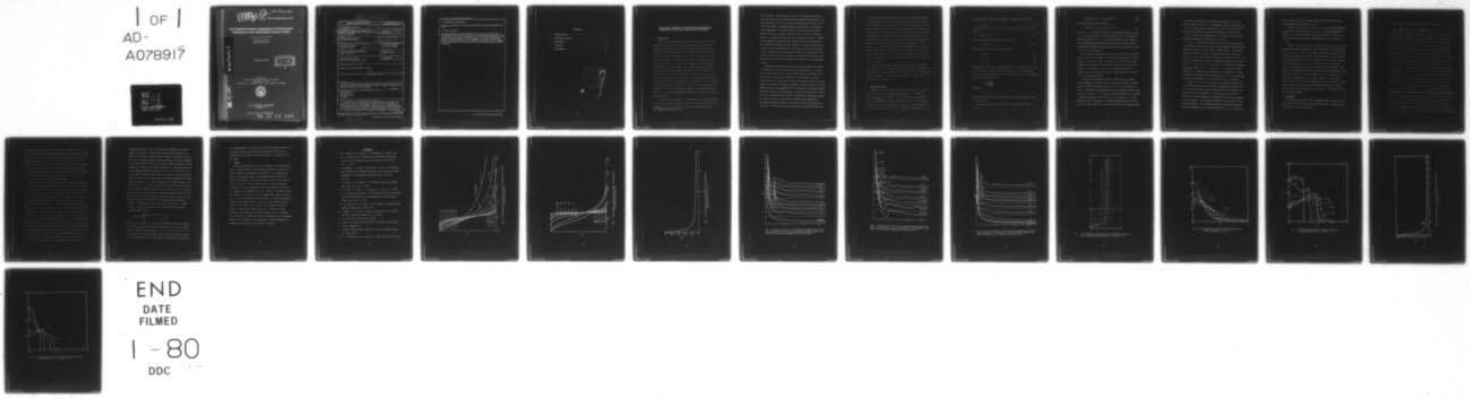

END
DATE
FILMED
1-80
DDC

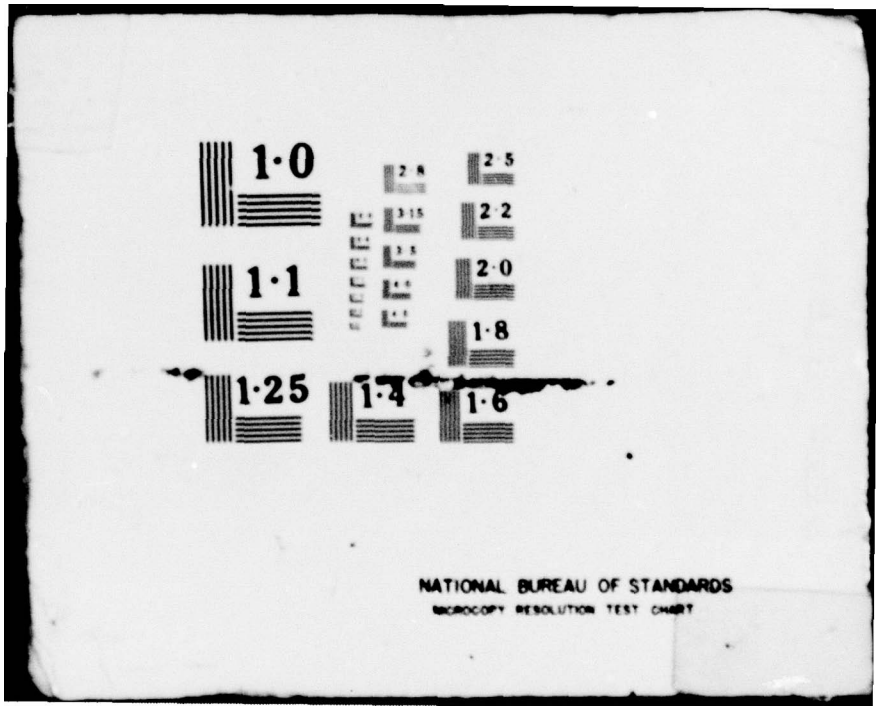
1·0
1·1
1·25
1·4
1·6
1·8
2·0
2·2
2·5
NATIONAL BUREAU OF STANDARDS
MICROCOPY RESOLUTION TEST CHART

NRL Memorandum Report 4129

Gas Channel Formation: Dependence of Hydrodynamic Phenomena on the Initial Radial Pressure Profile

MARTIN LAMPE AND SELIG KAINER

Plasma Theory Branch
Plasma Physics Division

November 30, 1979

Sponsored by
Defense Advanced Research Projects Agency (DoD)
ARPA Order No. 3718
Monitored by C. M. Huddleston Under Contract # N60921-79-WR-W0186

NAVAL RESEARCH LABORATORY
Washington, D.C.

14 NRL-MR-4129

SECURITY CLASSIFICATION OF THIS PAGE (When Data Entered)

REPORT DOCUMENTATION PAGE	READ INSTRUCTIONS BEFORE COMPLETING FORM
1. REPORT NUMBER: NRL Memorandum Report 4129	2. GOVT ACCESSION NO. / 3. RECIPIENT'S CATALOG NUMBER
4. TITLE (and Subtitle): 6 GAS CHANNEL FORMATION: DEPENDENCE OF HYDRODYNAMIC PHENOMENA ON THE INITIAL RADIAL PRESSURE PROFILE	5. TYPE OF REPORT & PERIOD COVERED: Interim report on a continuing NRL problem. / 6. PERFORMING ORG. REPORT NUMBER
7. AUTHOR(s): 10 Martin Lampe and Selig Kainer	8. CONTRACT OR GRANT NUMBER(s): 11 30 Nov 79
9. PERFORMING ORGANIZATION NAME AND ADDRESS: Naval Research Laboratory, Washington, DC 20375 — 12 27	10. PROGRAM ELEMENT, PROJECT, TASK AREA & WORK UNIT NUMBERS: NRL Problem 67R08-93B
11. CONTROLLING OFFICE NAME AND ADDRESS: Defense Advanced Research Projects Agency, Arlington, VA 22209	12. REPORT DATE: November 30, 1979 / 13. NUMBER OF PAGES: 26
14. MONITORING AGENCY NAME & ADDRESS (if different from Controlling Office): Naval Surface Weapons Center, White Oak, Silver Spring, Maryland 20910	15. SECURITY CLASS. (of this report): UNCLASSIFIED / 15a. DECLASSIFICATION/DOWNGRADING SCHEDULE

16. DISTRIBUTION STATEMENT (of this Report)

Approved for public release; distribution unlimited.

9 Memorandum rept.,

17. DISTRIBUTION STATEMENT (of the abstract entered in Block 20, if different from Report)

18. SUPPLEMENTARY NOTES

The views and conclusions contained in this document are those of the authors and should not be interpreted as representing the official policies, either expressed or implied, of the Defense Advanced Research Projects Agency or the U.S. Government.

(Continues)

19. KEY WORDS (Continue on reverse side if necessary and identify by block number)

Charged particle beam
Hydrodynamics
Gas channel formation
Hole boring

20. ABSTRACT (Continue on reverse side if necessary and identify by block number)

The hydrodynamic processes resulting from "instantaneous" heating of a cylindrical region of gas are studied by means of numerical integration of the fluid equations. Various initial over-pressures and radial profiles of initial pressure are considered. For very smooth radial profiles, e.g. the Bennett profile, the evolution is very simple: the gas expands radially, a single outgoing shock forms, the density at late times undershoots the value at pressure balance by only about 10% and then increases to pressure balance slowly, monotonically, and adiabatically. For profiles that are

(Continues)

DD FORM 1473 EDITION OF 1 NOV 65 IS OBSOLETE
S/N 0102-014-6601

SECURITY CLASSIFICATION OF THIS PAGE (When Data Entered)

251 950

JOB

18. Supplementary Notes (Continued)

This research was sponsored by the Naval Surface Weapons Center under Contract #N60921-79-WR-W0186.

20. Abstract (Continued)

more square in shape, or are sharply discontinuous, the evolution is much more complicated. A strong rarefaction typically occurs, of brief duration and in a narrow region about the axis. During the rarefaction, both the density and temperature fall well below the values at pressure balance. The rarefaction is abruptly terminated by an inward-propagating shock, followed by multiple density oscillations, which can form shocks for strong overpressures. The dependence of the time scales and strengths of the rarefactions and shocks on the initial overpressure and profile shape are calculated and discussed.

CONTENTS

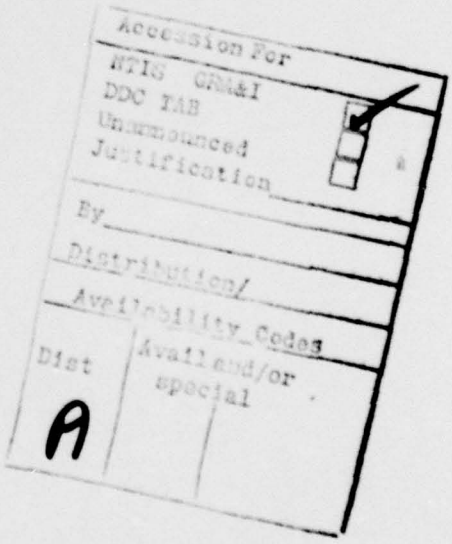

GAS CHANNEL FORMATION: DEPENDENCE OF HYDRODYNAMIC PHENOMENA ON THE INITIAL RADIAL PRESSURE PROFILE

I. Introduction

Several laboratories have recently studied the production of hot reduced density channels in air and other gases by pulsed directed energy sources such as electron beams,[1] pulsed lasers,[2] electrical discharges,[3] and exploding wires.[4] Such channels persist in pressure balance with the surrounding gas until they cool, typically for milliseconds and longer. All of the energy sources cited above typically have pulse durations ($\ll 1\,\mu$sec) short compared to the hydrodynamic response time of the heated gas. Thus the hydrodynamic response decouples from the energy deposition process, and can be treated as a one-dimensional initial value problem: the radial motion of an initially uniform-density gas with a given cylindrically symmetric initial temperature profile. Self-similar blast wave solutions to this problem, in closed form, are well-known,[5] but only for very large initial overpressures. In the range of greatest interest, overpressures ranging from two to 10^2 times the ambient pressure, numerical solutions are required in general.

We have previously examined[6] the hydrodynamics of channel formation for the special case of a Bennett initial radial overpressure profile, typical of a uniform gas heated by a self-pinched, mono-energetic

Note: Manuscript submitted October 6, 1979.

electron beam.[7] The evolution was found to be remarkably simple in that case, with the central heated region expanding adiabatically, and nearly monotonically, until it reaches pressure balance with the surrounding cool gas. The central density dips only about 10% (practically independent of the overpressure) below its value at pressure balance and then very slowly increases until it returns to pressure balance. No density oscillations occur during this process. A single shock propagates outward radially, heating the gas it overruns, and thus moderately reducing the final density in the radial wings of the channel and broadening the wings, but having no effect in the channel center. Formulas for the final density profile (including shock wave effects), and for the time evolution, were derived heuristically, and were found to agree well with numerical solutions of the hydrodynamic problem.

Heating profiles differing significantly from Bennett can result from several of the pulsed energy sources mentioned above. In particular, energy deposition by lasers through clean air breakdown occurs only when the laser intensity exceeds a sharp threshold; thus the central region of the pulse can heat the gas strongly, while the radial wings do not deposit any energy, leading to a nearly square or "top-hat" radial profile of gas temperature.[8] In this report, we present detailed numerical studies of the hydrodynamic evolution resulting from a variety of radial heating profiles, ranging from Bennett and Gaussian to square. Our results confirm the qualitative effects studied elsewhere[8] by approximate numerical methods, but are more extensive and numerically accurate. We find that heating profiles with a more square shape than

the Bennett profile typically lead to multiple oscillations (ringing) of the channel density. If the overpressure is strong, these oscillations can steepen into shocks, and one or more ingoing shocks can overrun the channel and reflect off the axis, in addition to the initial outgoing shock. For brief periods during these oscillations, a strong inward-propagating rarefaction wave drives both the density and the temperature on the channel axis to well below their final values (when the channel reaches pressure balance with the ambient gas). (For example, for a square profile and initial overpressure factor 23, the minimum channel density is 6% of the initial density, while the final density is 9% of the initial.) Thus, transient situations occur that are particularly favorable for applications where a cool, low density channel is desired.

In Section 2, we present the results of numerical calculations over a broad range of overpressures and radial profiles, emphasizing the dependence of density minima, shock characteristics, and time scales on these parameters. The results are interpreted in Sec. 3, and our conclusions are summarized in Sec. 4.

2. Numerical Results

We have used a one-dimensional (radial) fluid code to calculate the time evolution of the channel hydrodynamics for a variety of heating strengths and profiles. The code, which has been described previously,[9,10] performs finite-difference solutions of the equations of conservation of mass, momentum, and energy, using an Eulerian flux-corrected transport algorithm, which accurately resolves shocks. All

calculations and results are expressed in dimensionless variables,

$$\tilde{r} = r/a, \tag{1a}$$

the radial position scaled to the characteristic radius of the heated profile,

$$\tilde{v} = v/c_{so}, \tag{1b}$$

velocity scaled to the ambient gas sound speed,

$$\tilde{t} = c_{so}t/a, \tag{1c}$$

time scaled to the sound transit time, and

$$\tilde{\rho} = \rho/\rho_o, \tag{1d}$$

$$\tilde{P} = P/P_o, \tag{1e}$$

$$\tilde{T} = T/T_o, \tag{1f}$$

the density, pressure, and temperature, scaled to ambient values. Heat flow and radiative energy transfer typically occur on a much slower time scale than the hydrodynamic flow, and are omitted. For convenience, we hold the adiabatic index,

$$\gamma = \frac{\rho}{P}\left(\frac{dP}{d\rho}\right)_T , \tag{2}$$

constant at

$$\gamma = 7/5, \tag{3}$$

rather than modeling the detailed equation of state of any particular gas composition.

We parametrize the heating profiles as "generalized Bennett" profiles,

$$\tilde{P}\ (\tilde{r},\ \tilde{t} = 0) = 1 + P_o(1 + \tilde{r}^{\,n})^{-n} \qquad (4a)$$

and "generalized Gaussian" profiles,

$$\tilde{P}\ (\tilde{r},\ \tilde{t} = 0) = 1 + P_o \exp\ (-\tilde{r}^{\,-n}). \qquad (4b)$$

The value n = 2 corresponds to Bennett and Gaussian profiles, in Eqs. (4a) and (4b) respectively, and increasing values of n correspond to squarer profiles; for $n \to \infty$, both profiles approach step functions (but the generalized Gaussian profiles approach this limit faster). The generalized Bennett and Gaussian profiles are illustrated in Figs. 1 and 2 for a wide range of n.

For purposes of comparison with our previous work[6], we show here in Fig. 3 the time evolution of a deposition with the Bennett profile with $P_o = 37$, for early times. The density at the center decreases monotonically and smoothly (the only shock forms at $\tilde{r} = .8$ and runs outward). This result is typical for the Bennett distribution profile where no ringing of the central channel density is observed and no ingoing shock appears.

The evolution becomes increasingly complex as one considers initial temperature profiles that are squarer then Bennett, as shown in Fig. 4, where the time evolution of $\tilde{\rho}\ (\tilde{r} = 0)$ is plotted for a series of generalized Gaussian profiles with increasing values of the index n, all with $P_o = 37$. Even for a Gaussian profile (n = 2), there is a gentle maximum of $\tilde{\rho}\ (\tilde{r} = 0, \tilde{t})$ at $\tilde{t} = 1$, and for $n \geq 3$, this maximum clearly corresponds to an inward-propagating shock striking the axis. The strength of this shock increases for increasing values

of n, until (surprisingly) it reaches a maximum at $n \approx 10$, with density jump by a factor ≈ 7.3, and weakens slightly to density jump ≈ 4.6 for still squarer profiles with $n \geq 10$. (The fact that the density jump exceeds the maximum Rankine-Hugoniot value, 6, for $\gamma = 7/5$, is due to the combined effect of the inward shock and the subsequent outward shock reflected off the axis.)

For $n > 3$, the initial pressure profile is sufficiently square that no motion occurs at $\tilde{r} = 0$ until a well-defined rarefaction wave, traveling at the local sound speed, reaches the axis. The density then falls rapidly, reaching a minimum value that is as low as $\tilde{\rho} = 0.06$ for $P_o \geq 10$, just before the inward shock reaches the axis. For purposes of comparison, adiabatic expansion would reduce the density only to $\tilde{\rho} = 0.2$, for $P_o = 10$. The duration of the density minimum is quite short, about $\delta\tilde{t} \approx 0.1$. Also, for $n \geq 3$, a weak but definite ringing of the channel occurs subsequently, the amplitude of which increases as the heating profile becomes squarer. Such ringing might possibly have some impact on channel stability and cooling rate.

In Fig. 5, $\tilde{\rho}\ (\tilde{r} = 0, \tilde{t})$ is plotted, for various overpressures P_o for an essentially square radial profile (generalized Gaussian with $n = 50$). We see that an initial ingoing shock is well formed over the entire range of pressure P_o. The arrival time on axis is a function of the overpressure P_o but appears to be nearly independent of the squareness. The strength of the shock and the value of the density minimum for the preceding rarefaction is strongly dependent upon the squareness but only weakly dependent on P_o. In addition we

see from Fig. 5 as P_o is increased a second density maximum arises which steepens into a shock for $P_o \geq 56$.

A series of plots in Fig. 6 of $\rho(\tilde{r} = 0, t)$ for generalized Bennett profiles with various values of n but at $P_o = 74$ shows phenomenology similar to that seen with generalized Gaussian profiles in Fig. 4. We see here that the second density maximum steepens into a shock for $n \geq 4.5$.

In Fig. 7, we show a series of snapshots at different times of the instantaneous density profile $\tilde{\rho}(\tilde{r})$, for a generalized Gaussian profile with $n = 50$ and $P_o = 74$. For the latter case, we note particularly the profile $\tilde{\rho}(\tilde{r})$ during the transient density minimum, just before the inward shock arrives on axis. The low density "hole" on axis is rather narrow, extending only to $\tilde{r} \approx 0.3$, and its duration is only about $\delta\tilde{t} \approx 0.1$, as the hole is abruptly closed by the incoming shock. The depth of this minimum depends quite strongly upon the squareness of the profile (the index n), as seen in Fig. 4, but is quite insensitive to the initial overpressure as can be seen from Fig. 5. Thus a deep density channel can be produced, momentarily, even by a relatively weak beam. However, this economy of means might be difficult to use for practical applications, because of the brevity of its duration and the precise timing required.

3. Discussion

We have shown previously[6] that the channel density profile at late times, when the channel reaches pressure balance with the ambient gas, is defined by the set of equations

$$\tilde{\rho}\,(\tilde{r},\,\tilde{t}=\infty) = [\tilde{P}\,(\tilde{r}_o(\tilde{r}),\,\tilde{t}=0)]^{-1/\gamma}\,\exp\,[-\Delta S(\tilde{r})/c_v] \qquad (5a)$$

$$\tilde{r}^2 = \int_o^{\tilde{r}_o^2} [\tilde{P}(r')]\,1/\gamma\,\exp\,(\Delta S(\tilde{r})/c_v)\,2r'\,dr' \qquad (5b)$$

where $\tilde{r}_o$ is the Lagrangian coordinate of a particular fluid element, i.e., the location at $\tilde{t}=0$ of the fluid element that is at $\tilde{r}$ at $\tilde{t}=\infty$, and $\Delta S(\tilde{r})$ is the increase in entropy density due to shocks that have traversed this fluid element. There is no general formula for $\Delta S(\tilde{r})$, but in Ref. 6 we presented heuristic formulas for $\Delta S(\tilde{r})$ that accurately described the outgoing shock in the case of a Bennett profile, and in fact are reasonably accurate for the first outgoing shock in the general case. For the Bennett profile, $\Delta S = 0$ for the central channel, since there is only a single, outgoing shock, which originates at $\tilde{r} \approx 0.8$; thus the central channel is formed strictly by adiabatic expansion, and the main effect of the shock is to broaden the channel wings. Furthermore, the time evolution is very smooth and simple for the Bennett profile, with the density decreasing monotonically to about 10% below the value given by Eq. (5), and then returning slowly to that value.

For profiles of squarer shape, we have seen that the hydrodynamic evolution is more complicated, i.e.: (i) A strong rarefaction reduces the density to a value well below that of Eq.(5),for a brief period when $\tilde{t} \approx 0.7$. The temperature is also at a minimum at this time. (ii) Both the density and temperature abruptly increase when an inward shock hits the channel axis. This shock can be quite strong. (iii) There is a good deal of subsequent structure in the time evolution. In particular, the incoming shock reflects off the axis, and for strong overpressures,

a second ingoing shock (which is always weak) is observed. (iv) The channel density at late times when pressure balance is achieved is given by Eq. (5) and is significantly decreased below the adiabatic value by the entropy increase ΔS due to the first ingoing shock, e.g., $\tilde{\rho}(\tilde{r} = 0, \tilde{t} = \infty) = 0.044$ for squarish profiles with $P_o = 74$ as compared to an adiabatic value, 0.053. The channel temperature at late time (determined by pressure balance) is always much larger than the temperature during the first density minimum, e.g. $\tilde{T} = 63$ at $\tilde{t} = \infty$ while $\tilde{T} = 21$ at the time of the first density minimum.

It is striking that these effects do not necessarily require that the initial overpressure profiles have a sharp "corner" or discontinuity, but occur also for profiles that are only moderately squarer in shape than the Bennett profile, e.g. the generalized Bennett with $n = 4.5$ (see Fig. 1) or the generalized Gaussian with $n = 3$ (see Fig. 2). In fact the inward shock is stronger for the generalized Gaussian with $n = 10$ than for squarer profiles with $n \gtrsim 30$. The strong rarefaction and inward shock seem to be due primarily to the presence of a relatively flat central region of the profile. This can be understood as follows. In a uniform medium, a pressure pulse steepens to a shock as a result of nonlinear effects: the temperature, and therefore the local sound speed, is larger within the pulse, and therefore the center of the pulse tends to overtake the front. This tendency is reinforced if the pressure pulse is propagating down a temperature gradient, but is weakened if the pulse must propagate toward a region of increasing temperature; in the latter case, the front of the disturbance tends to run away from disturbance. As a result, waves (rarefactions or compressions) propagating up a

temperature gradient tend to be gentle, and compressions tend not to steepen into shocks. Smooth radial pressure profiles such as the Bennett profile have a non-zero initial temperature gradient except on axis, and a temperature gradient persists during the initial expansion of the heated region (see Fig. 8). Thus one expects subsequent inward-propagating features to be slow and gentle, as is indeed the case: the central density decreases smoothly, over a very long time scale, to a value slightly below its final value, and returns, even more slowly, to pressure balance. On the other hand, the modified Bennett and Gaussian distributions with $n \geq 5$ have a pronounced flat central region (but no real corner until n is much larger), which persists and is conducive to strong inward propagating rarefactions and shocks at early times (see Fig. 9). For very square profiles (generalized Gaussian with $n > 10$), the shock strength decreases slightly. On the other hand, an initial over-pressure profile in the form of a truncated Bennett profile does result in an ingoing shock and other features typical of a "square" profile. In Fig. 10, we exhibit the evolution resulting from an initial heating profile

$$P(\tilde{r},\tilde{t}=0) = \begin{cases} 1 + P_o\,(1+\tilde{r}^2)^{-2}, & \tilde{r} \leq \tilde{r}_o \\ 1, & \tilde{r} > \tilde{r}_o \end{cases},$$

with $P_o = 74$, and $\tilde{r}_o = 0.8$. Such a profile does not have an initially flat central region, but does have a discontinuity out on the radial wings. However, we see in Fig. 11 that a flat central temperature profile does evolve at a later time, due to the rarefaction wave running in from the discontinuity, and that this is followed by the formation

of an ingoing shock. Thus the type of time development discussed in this paper results from an initial overpressure profile that is characterized by either a flat central region or a discontinuity at any point.

4. Summary

We have concluded that if a gas is heated, by a directed energy source, instantaneously on a hydrodynamic time scale, in such a way that the initial overpressure profile $\tilde{P}(\tilde{r},\tilde{t}) = 0)$ is either flat-topped or sharp-edged, then the subsequent expansion will not be smooth and adiabatic in the central region, as it is for a Bennett pressure profile.[6] Rather, there will be a strong rarefaction, followed by an inward propagating shock, and subsequent oscillation or "ringing" of the channel will occur. There is a transient period, just before the arrival of the first inward shock, when the central channel is at low temperature and low density. For square deposition profiles, the channel density at late time, when pressure balance with the surrounding gas is achieved, is decreased by the shock heating to about 80% of what it would be for adiabatic channel formation. The strength of the shock depends mainly on the shape of the profile. The time scale for the rarefaction and shock depends mainly on the strength of the overpressure. These dependences are extensively illustrated in the numerical solutions.

REFERENCES

1. R. J. Briggs, T. C. Clark, T. J. Fessenden, R. E. Hester, and E. J. Lauer, Proc. 2nd International Conference on High Power Electron and Ion Beam Research and Technology, October 1977, Vol. I, p.319.
2. D. Koopman, J. R. Greig, R. Pechacek, A. Ali, I. M. Vitkovitsky and R. Fensler, Proceedings of the XIVth International Conference Phenomena in Ionized Gases, Grenoble, France, July 1979, p.C7-419.
3. J. R. Vaill, D. A. Tidman, T. D. Wilkerson, and D. W. Koopman, Appl. Phys. Lett. 17, 20 (1970).
4. P. A. Miller, L. Baker, J. R. Freeman, L. P. Mix, J. W. Ponkey, T. P. Wright, Proceedings of 2nd International Topical Conference on High Power Electron and Ion Beam Research and Technology, October 1977, Vol. I, p.393.
5. L. D. Landau and F. M. Lifshitz, Fluid Mechanics (Addison-Wesley, Reading, Massachusetts, 1966, p.393.
6. M. Lampe, H. H. Szu and S. Kainer, "Hydrodynamics of Gas Channel Formation," NRL Memo. Report 4073 (in press).
7. E. P. Lee, Phys. Fluids 19, 60 (1976).
8. G. Weyl, R. Patrick, and R. Ruquist, Avco Everett Laboratories, private communication.
9. J. Boris, Computer Phys. Comm. 12, 67 (1976); NRL Memo. Report 3237 (March 1976).
10. D. G. Colombant and J. H. Gardner, J. Comp. Phys. 22, 389 (1976).

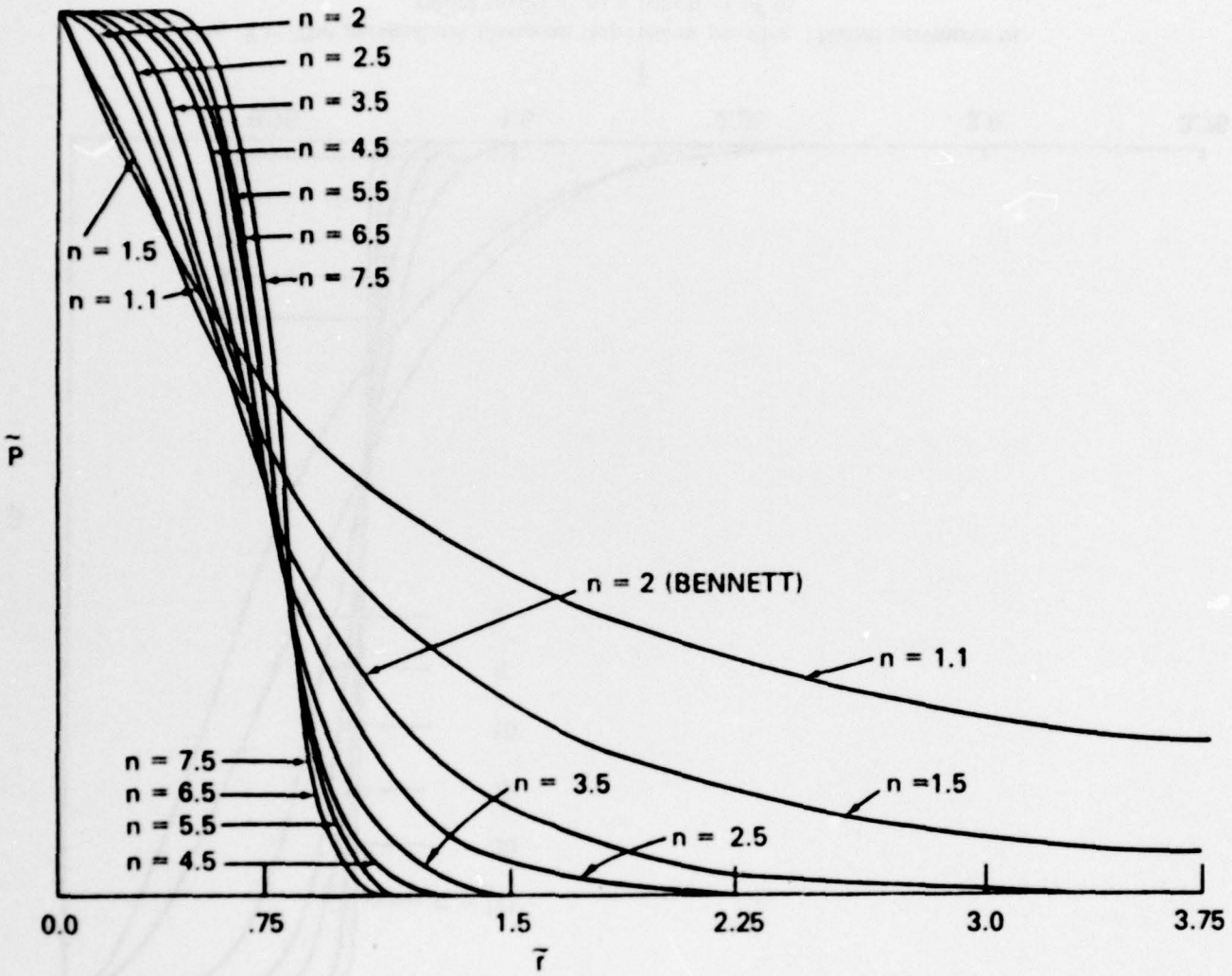

Fig. 1 — The generalized Bennett deposition profiles. Initial pressures vs radial position as a function of n.

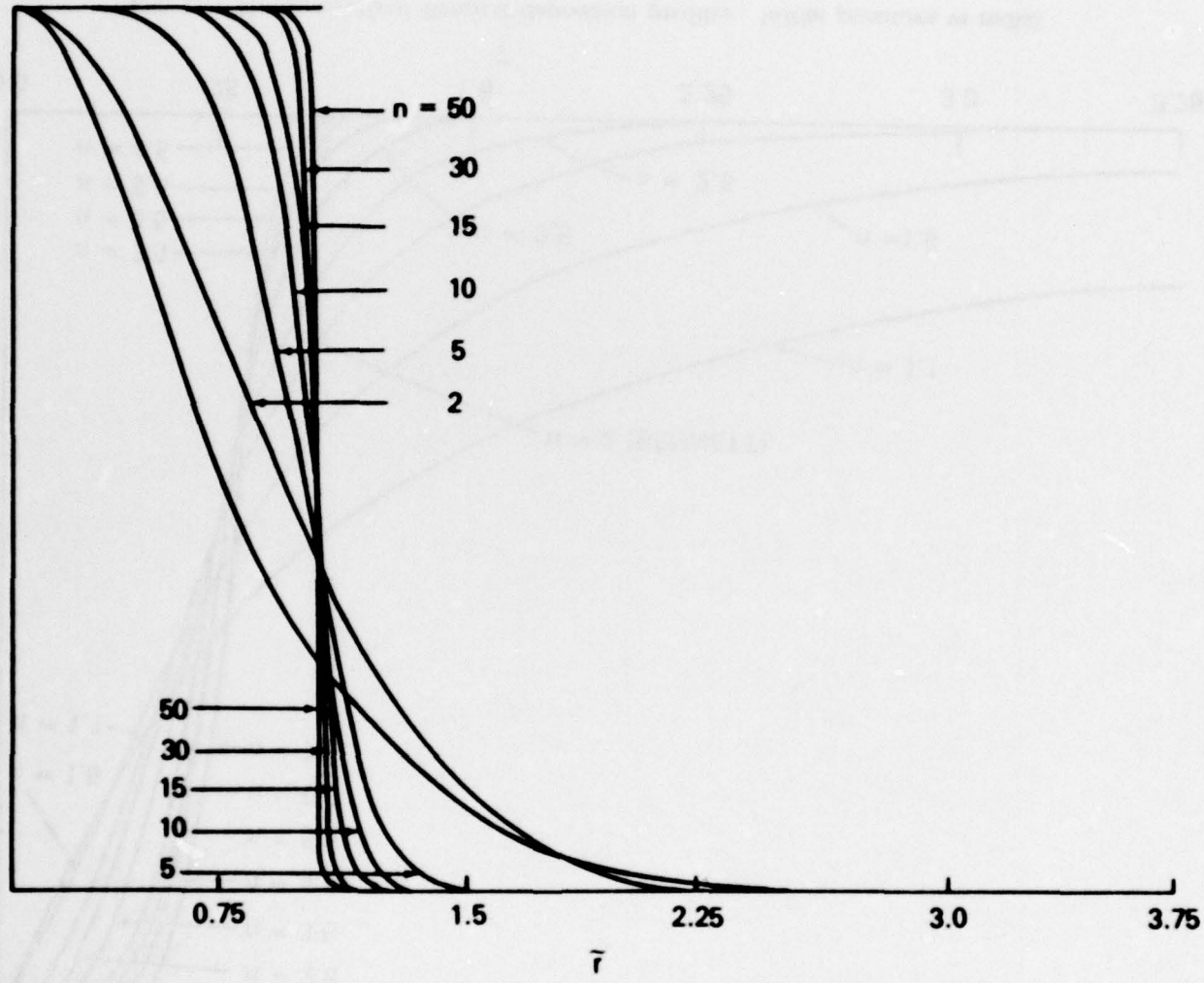

Fig. 2 — The generalized Gaussian deposition profiles. Initial pressures vs radial position as a function of n.

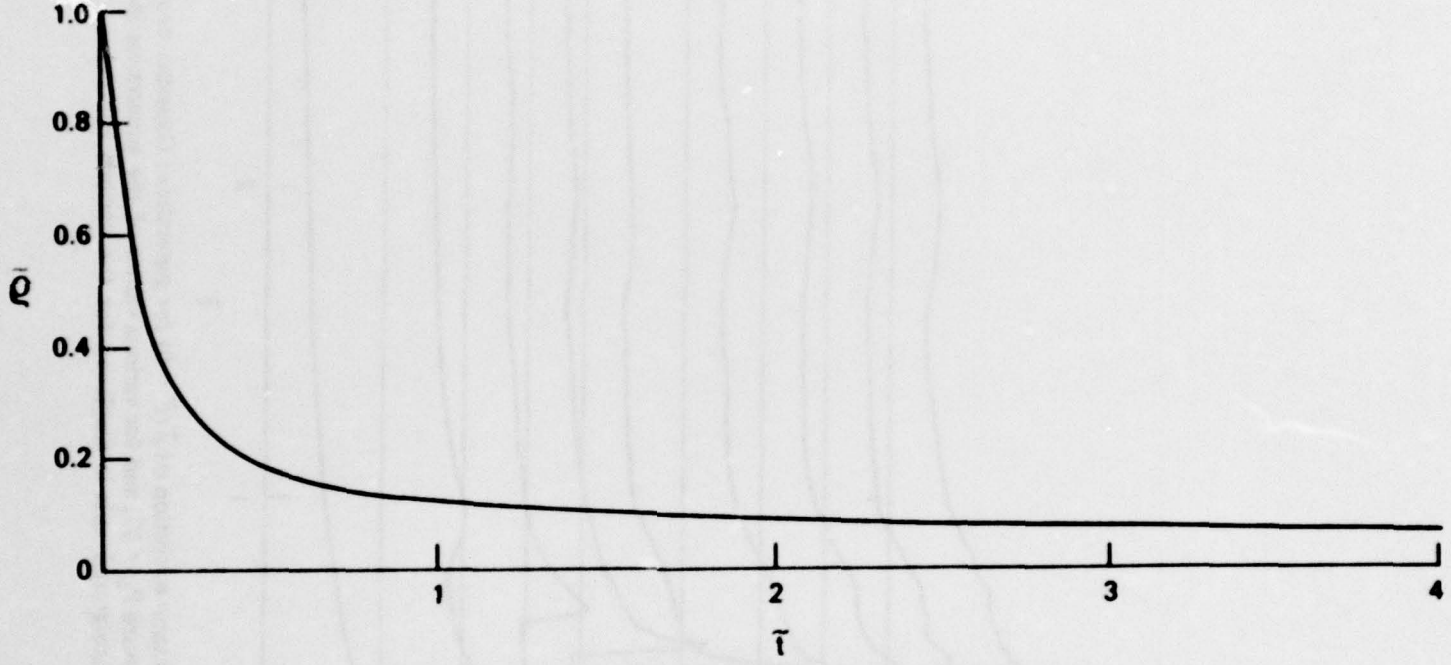

Fig. 3 — The time evolution of on-axis density for an initial Bennett deposition profile with $P_o = 37$

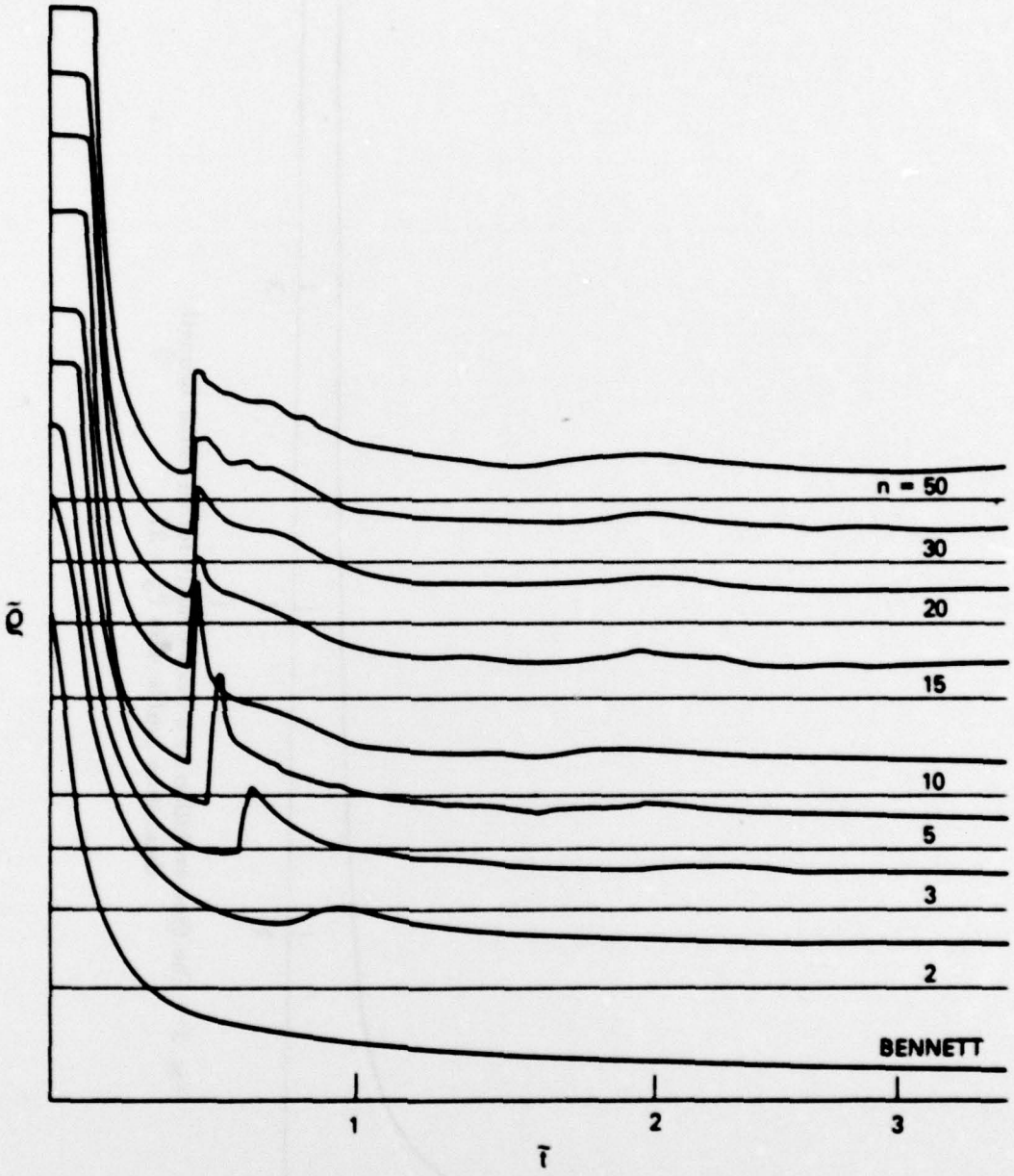

Fig. 4 — The time evolution of $\tilde{\rho}(\tilde{r} = 0)$ for generalized Gaussian heating profiles with overpressure $P_o = 37$, and for various values of the squareness index n. For clarity, the horizontal axis is displaced for the various curves.

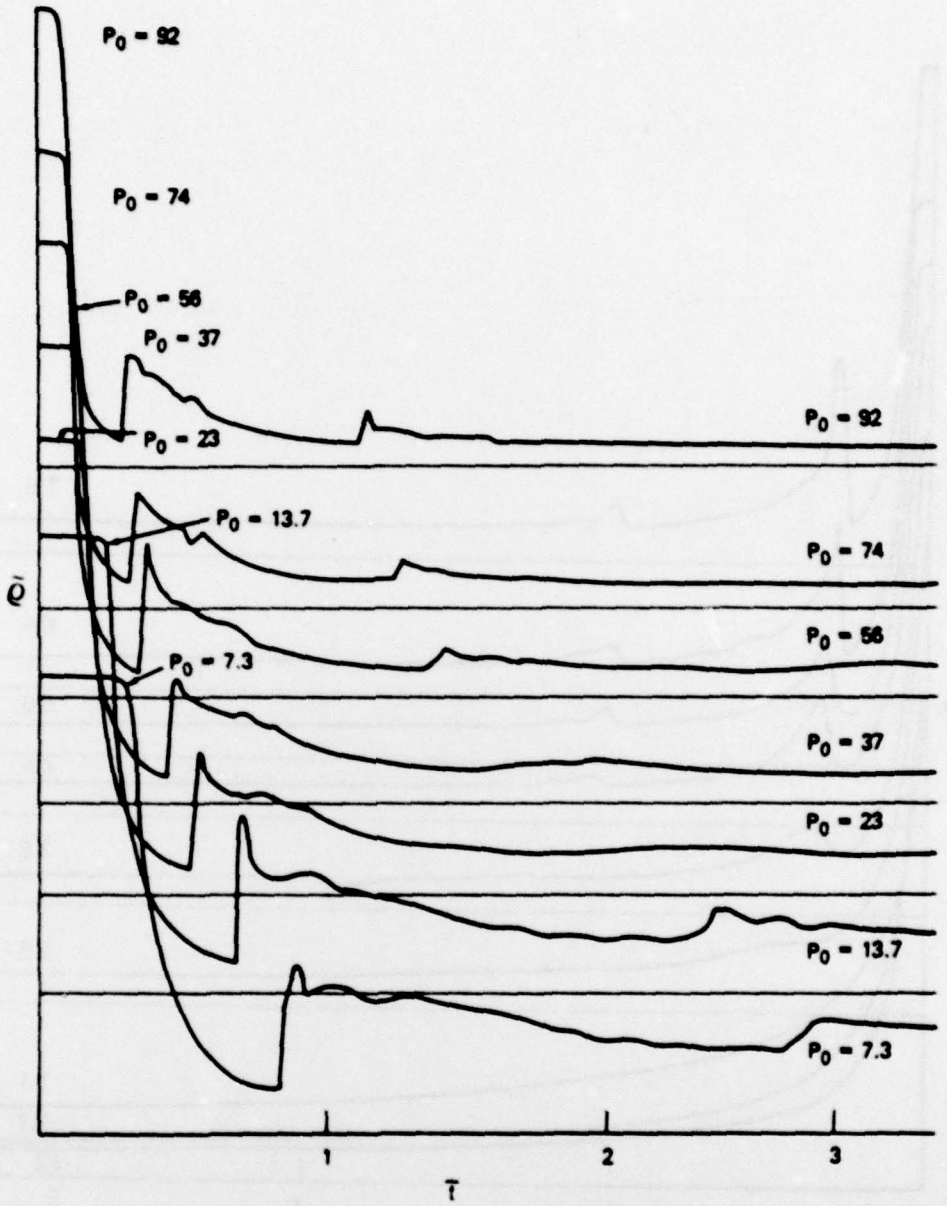

Fig. 5 — The time evolution of $\tilde{\rho}(\tilde{r} = 0)$ for generalized Gaussian heating profiles with n = 50 (nearly square), and for various values of the overpressure P_o. For clarity, the horizontal axis is displaced for the various curves.

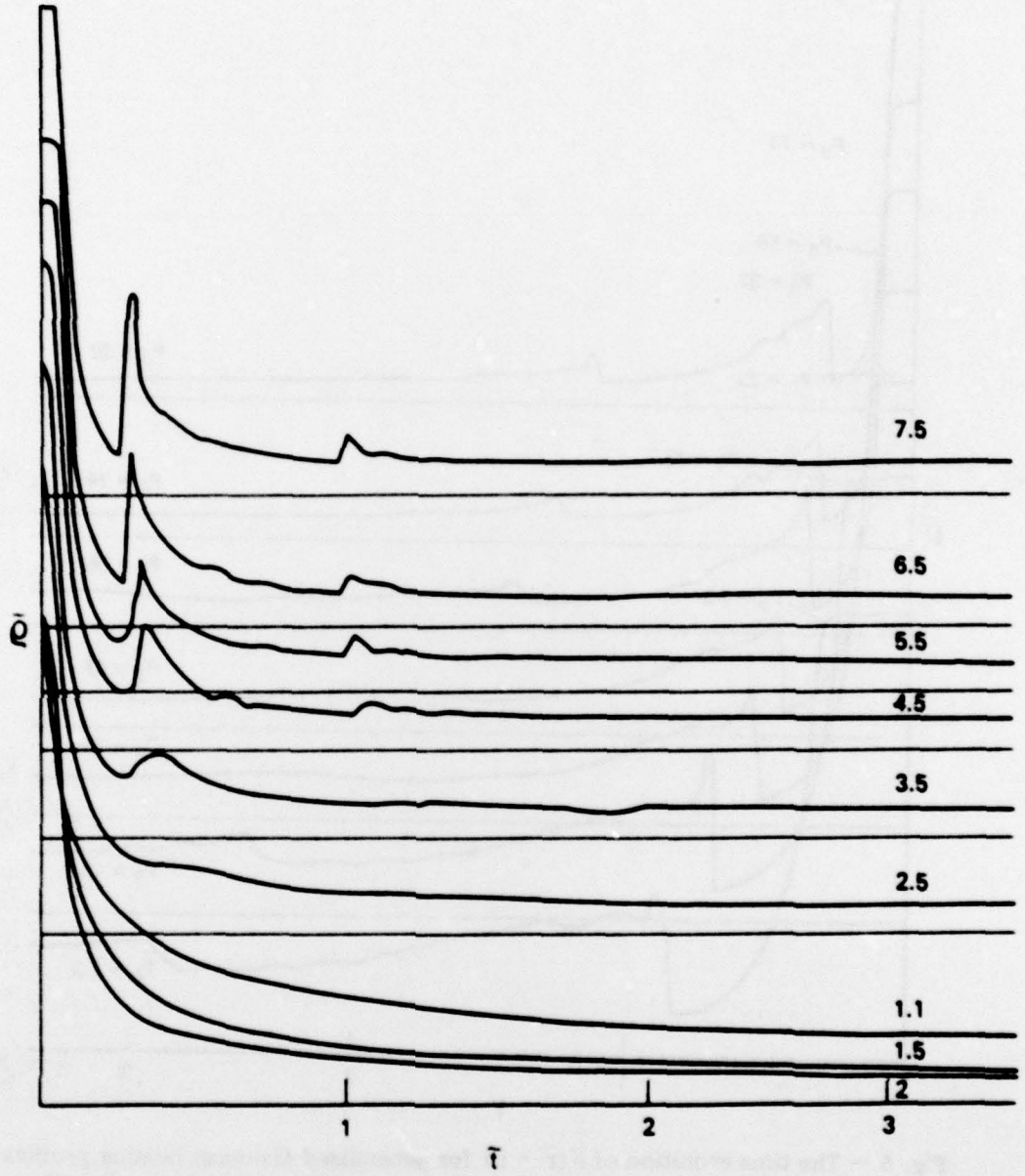

Fig. 6 — The time evolution of $\tilde{\rho}(\tilde{r} = 0)$ for generalized Bennett heating profiles with overpressure $P_o = 74$, and for various values of the squareness index n. For clarity, the horizontal axis is displaced for the various curves.

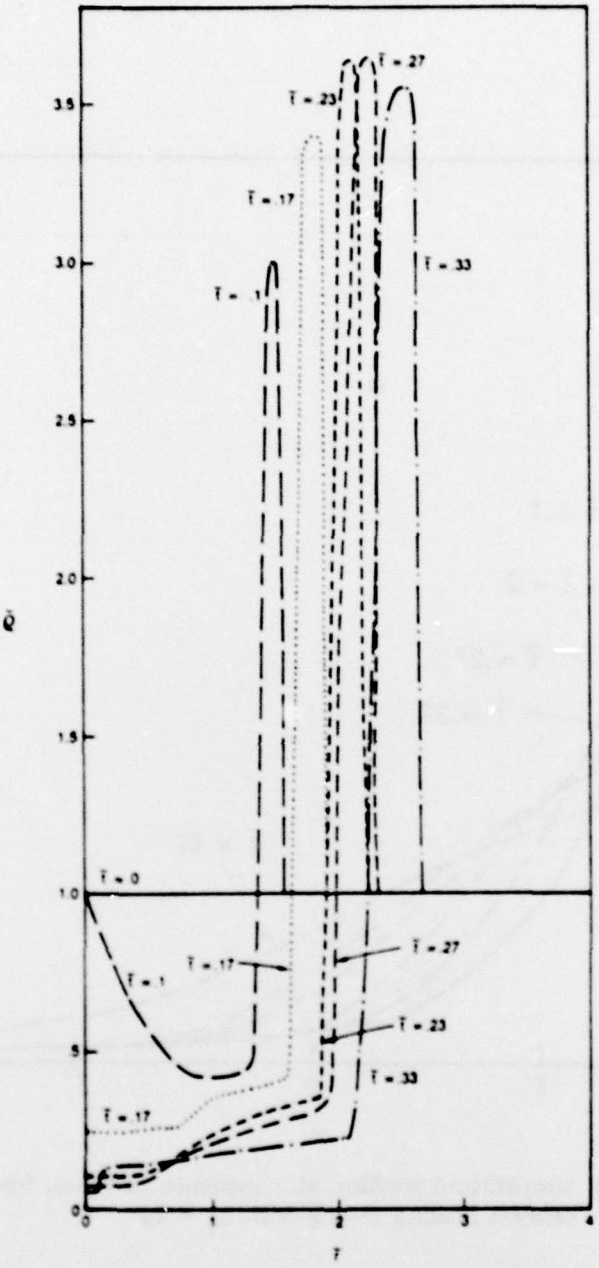

Fig. 7 — The instantaneous density profile $\tilde{\rho}(\mathbf{r})$, at a sequence of times, for a generalized Gaussian heating profile with n = 50 and P_o = 74

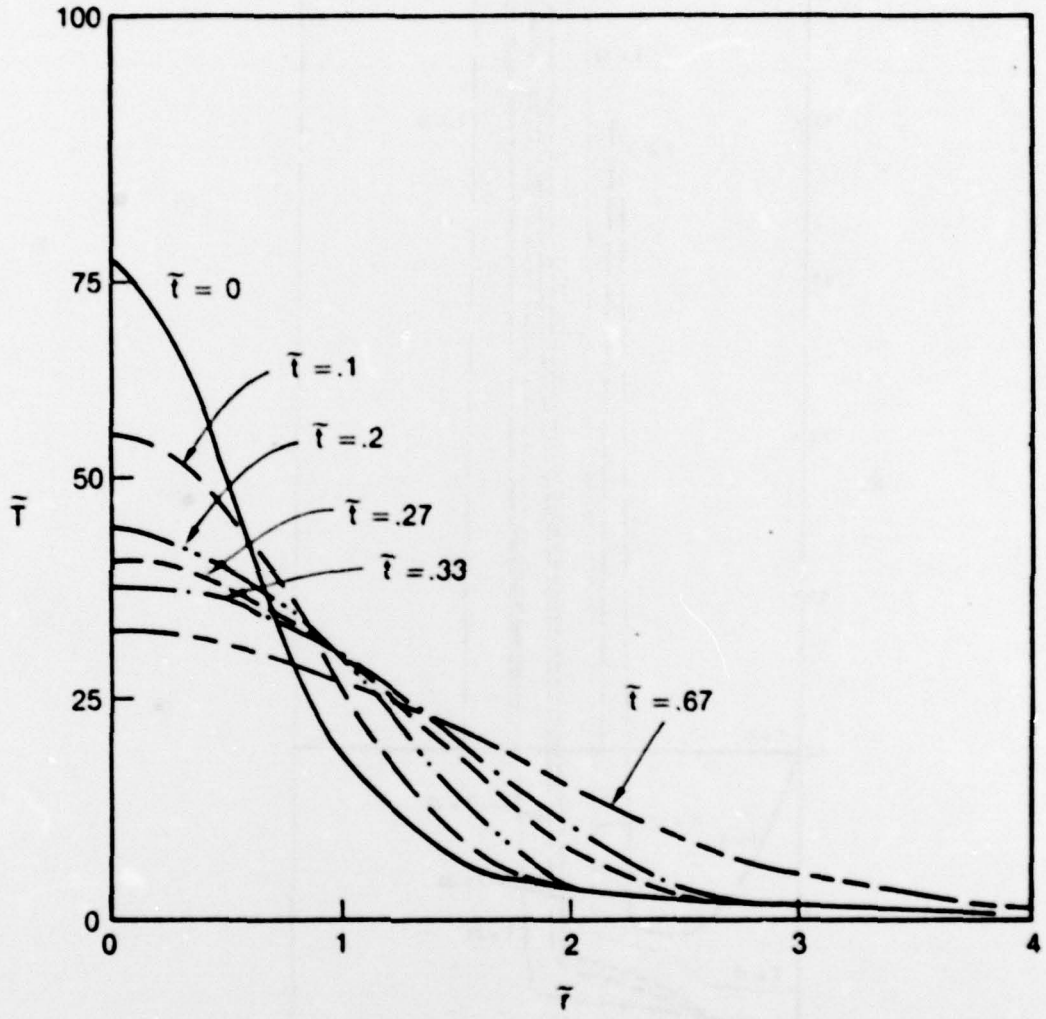

Fig. 8 — Radial temperature profiles, at a sequence of times, for the Bennett heating profile with $P_o = 74$

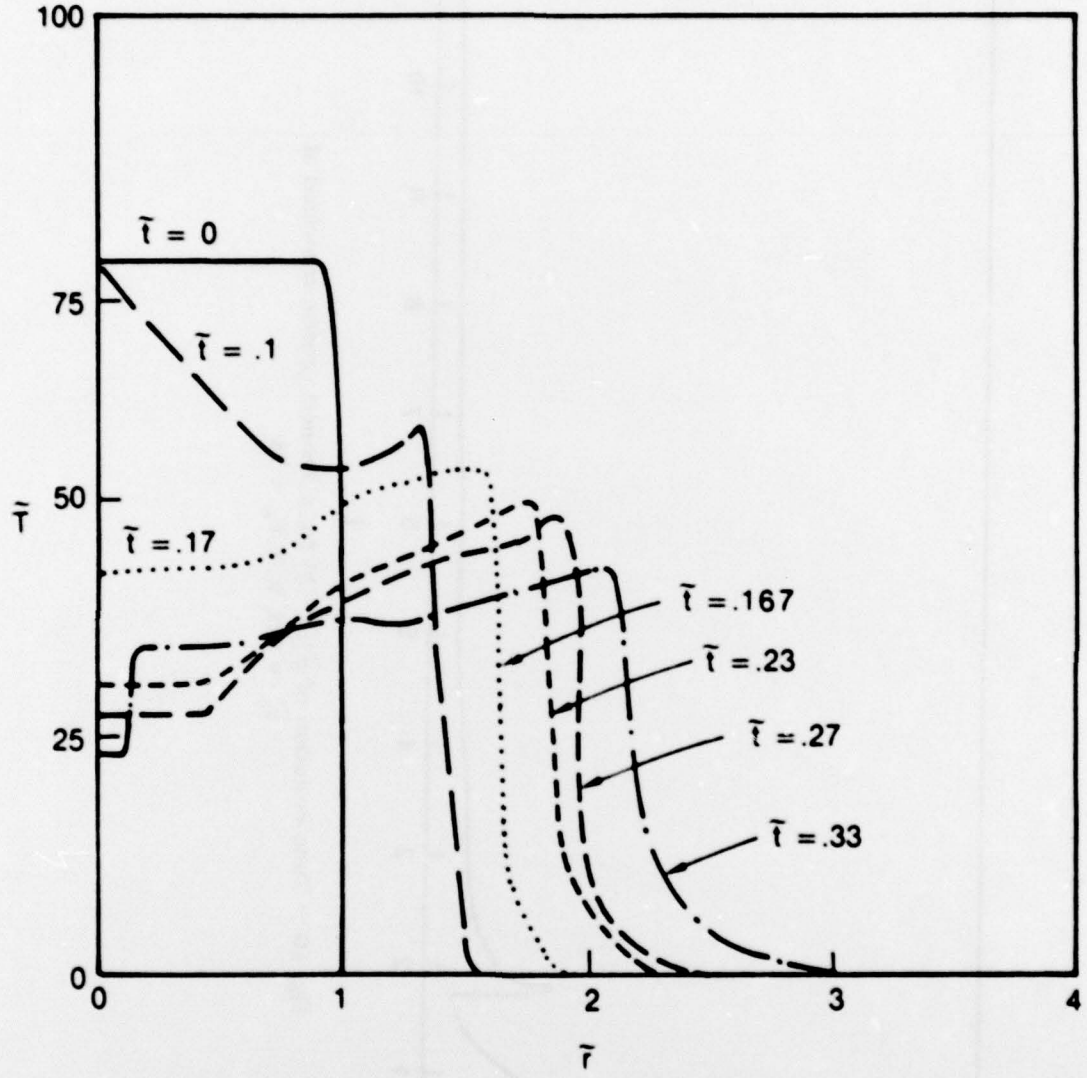

Fig. 9 — Radial temperature profiles, at a sequence of times, for a generalized Gaussian with n = 50 and P_o = 74

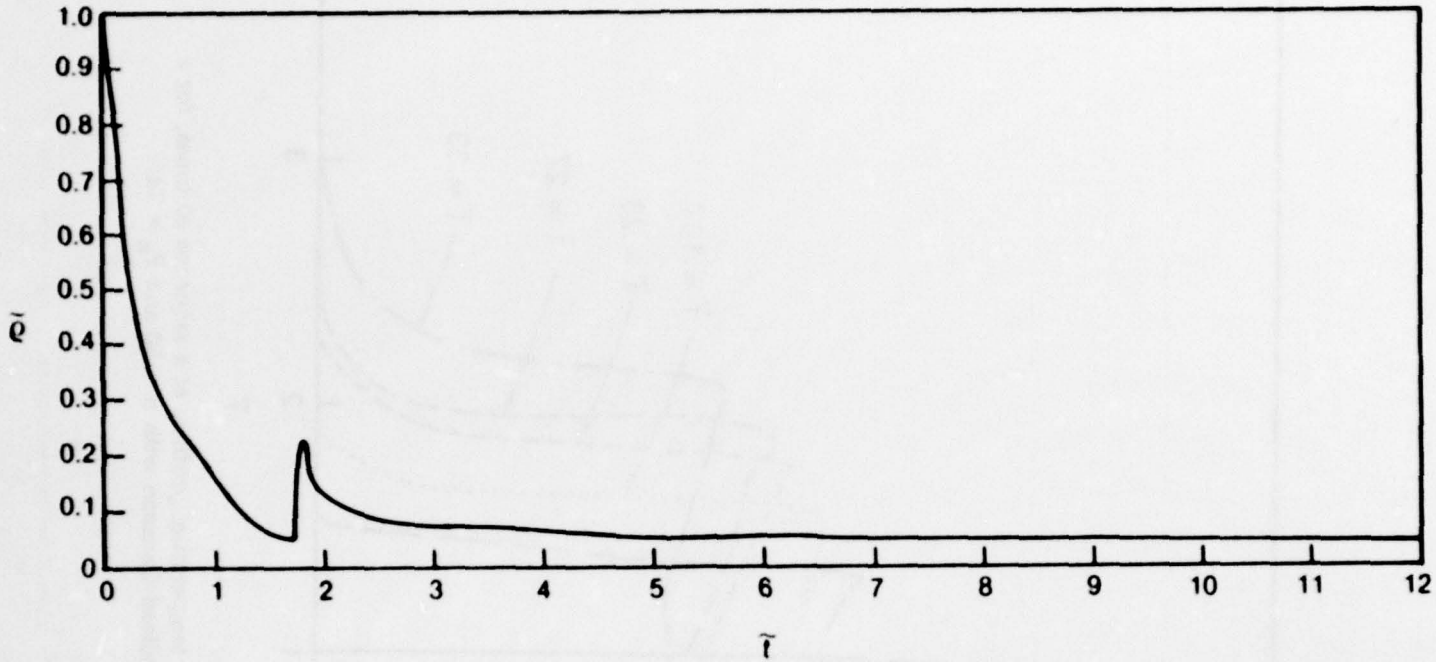

Fig. 10 — Time evolution of $\tilde{\rho}(\tilde{r} = 0)$ for a Bennett profile, truncated at $\tilde{r}_o = 0.8$, with $P_o = 74$

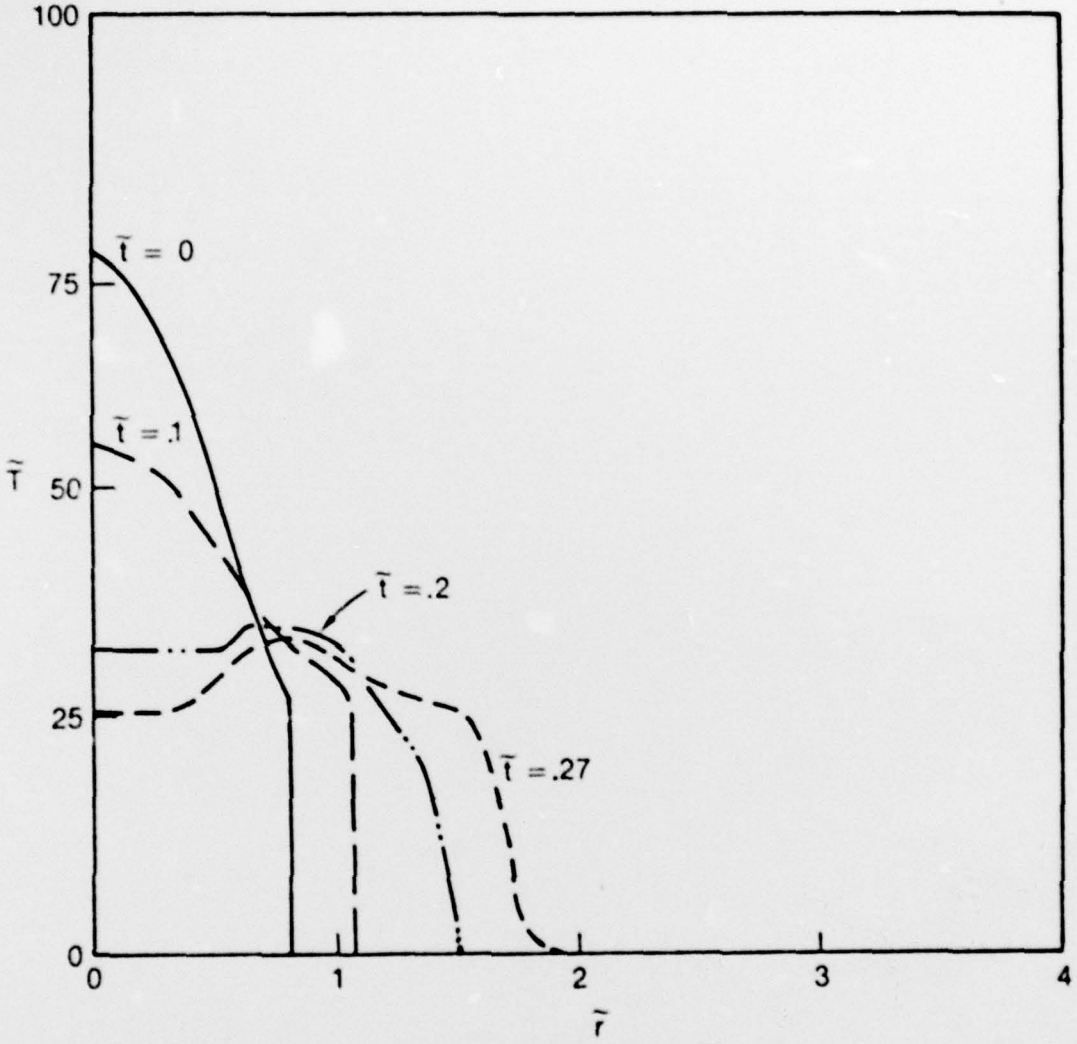

Fig. 11 — Radial temperature profiles, at a sequence of times, for a Bennett profile, truncated at $\tilde{r}_o = 0.8$, with $P_o = 74$